



## Integrating Pressure and Fractional Flow Data in Reservoir Modeling With Fast Streamline-Based Inverse Method

Xian-Huan Wen, SPE, Stanford University, Clayton V. Deutsch, SPE, University of Alberta, and A. S. Cullick, SPE, Mobil Upstream Strategic Research Center

Copyright 1998, Society of Petroleum Engineers, Inc.

This paper was prepared for presentation at the 1998 SPE Annual Technical Conference and Exhibition held in New Orleans, USA., 27-30 September 1998.

This paper was selected for presentation by an SPE Program Committee following review of information contained in an abstract submitted by the author(s). Contents of the paper, as presented, have not been reviewed by the Society of Petroleum Engineers and are subject to correction by the author(s). The material, as presented, does not necessarily reflect any position of the Society of Petroleum Engineers, its officers, or members. Papers presented at SPE meetings are subject to publication review by Editorial Committees of the Society of Petroleum Engineers. Permission to copy is restricted to an abstract of not more than 300 words. Illustrations may not be copied. The abstract should contain conspicuous acknowledgement of where and by whom the paper was presented. Write Librarian, SPE, P.O. Box 833836, Richardson, TX 75083-3836, U.S.A., fax 01-972-952-9435.

### Abstract

Generation of a reservoir model's spatial permeability distribution directly from historical multiple-well pressure and fractional flow rate data requires an inverse solution of the flow equations. This computation generally utilizes a gradient method to solve the minimization problem. A previously reported geostatistically-based inverse sequential self-calibration (SSC) technique has been shown to significantly reduce the computer time as compared to full inversion solutions and to yield excellent results for single-phase pressure.

In this paper we extend the SSC to jointly invert multiple well pressure and multiphase fractional flow data by: (1) adapting a fast streamline simulator for the forward flow solution; and (2) implementing a new method for computing the sensitivity coefficients for fractional flow rate. The method is fast and robust, and an important consequence of the method is that the spatial correlation structure is honored through the kriging equations in the SSC. This leads to well-behaved objective functions with low final values and preserves the prior model spatial characteristics.

The paper demonstrates the extended SSC for generating permeability realizations from production data using a synthetic reservoir model. The paper systematically compares the quality of the production data matches for inversion of pressure data alone, fractional flow rate data alone, and the combination of fractional flow rate and pressure data. For the synthetic model, pressure data alone provides coarse information primarily near the wells, whereas the fractional flow data provide more information on interwell spatial reservoir permeability. Inverting

pressure and fractional flow data jointly lead to significant improvement of the representation of reservoir heterogeneity and reduction in uncertainty. The paper shows that the accuracy of reservoir performance predictions at wells can be dramatically improved by building the models using the historical production data from those wells. However, if only production data have been used to build a model, the results also indicate that the prediction capability may be limited for new wells drilled in areas outside the influence region of existing wells or under flow or well conditions different from those used for the inversion. Future research directions are discussed at the end.

### Introduction

Reliable predictions of future reservoir performance require reservoir models that honor *all* available data including conceptual geological data, seismic data, core data, well log data, DST/RFT data, well test data, and historical production data. Each source of data carries information, at different scales and with varying precision, related to the true distribution of petrophysical and fluid properties in the reservoir. The challenge of reservoir characterization is to integrate all data sources.<sup>8</sup> Integrating all the available data *by construction* in numerical geological models will improve the predictive power of the models and make it possible for reservoir engineers to more quickly perform flow simulation studies. The production data is particularly important due to its close relationship to what we want to predict: fractional flow rates, pressures and recovery factors for example. In the proposed modeling scheme of Gouveia et al,<sup>8</sup> the production data is inverted to a coarse-scale permeability representation which is then combined with the seismic and other data through an optimization procedure to build the finer-scale reservoir model.

The procedure for generating a permeability model from production data usually begins with an inverse technique because the data are non-linearly related with reservoir permeability through the flow equations.<sup>10,12,13,18</sup> An iterative geostatistically-based inverse technique, called the self-calibration (SSC) method, has been developed and previously shown to be quite efficient for constructing multiple equiprobable reservoir models that honor single phase historical pressure data.<sup>4,7,17,19</sup> The unique features of the SSC algorithm are: (1)

concept of master point that reduces the parameter space to be estimated in the optimization process; (2) propagation through kriging that accounts for spatial correlation of permeability perturbations; and (3) fast computation of sensitivity coefficients of pressure within the single-phase flow simulation run.

Application of the SSC requires a variogram model that defines the propagation of the permeability perturbations. Integration of historical single phase pressure data was shown important for identifying large scale trends of permeability variation in reservoir models, particularly the high permeability channels or low permeability barriers and variations near wellbores.<sup>16,17,22,23</sup> Historical pressure data may also be inverted to derive spatially varying probability distributions of pay-facies proportion using the SSC method.<sup>20</sup>

In this paper, we extend the SSC technique to integrate multiple phase production data: the fractional flow rate data, such as watercut or GOR from production wells. A streamline-based multiphase flow simulator<sup>1,2,3,14,15</sup> is adapted for fast flow simulation. Also the 1D analytical streamline solution is utilized for fast calculation of sensitivity coefficients of fractional flow rate and thus for fast inversion for the reservoir properties. The objective function to be minimized in the extended SSC is in the form of:

$$O = \sum_{w_p=1}^{n_{w_p}} \sum_{t_p=1}^{n_{t_p}} W_p(w_p, t_p) [\hat{p}(w_p, t_p) - p(w_p, t_p)]^2 + \sum_{w_f=1}^{n_{w_f}} \sum_{t_f=1}^{n_{t_f}} W_f(w_f, t_f) [\hat{f}(w_f, t_f) - f(w_f, t_f)]^2 \quad (1)$$

where  $\hat{p}(w_p, t_p)$  and  $p(w_p, t_p)$  are the observed and simulated pressure at well  $w_p$  at time  $t_p$ .  $\hat{f}(w_f, t_f)$  and  $f(w_f, t_f)$  are the observed and simulated fractional flow rate at well  $w_f$  at time  $t_f$ .  $W_p(w_p, t_p)$  and  $W_f(w_f, t_f)$  are weights assigned to pressure and fractional flow rate data at different wells and at different time.  $n_{w_p}$  and  $n_{w_f}$  are the number of wells that have pressure and fractional flow data.  $n_{t_p}$  and  $n_{t_f}$  are the number of time steps for the observed pressure and fractional flow data.

A gradient method is used to minimize the objective function, which requires the sensitivity coefficients (derivatives) of pressure and fractional flow of wells at observed time steps with respect to the permeability changes at the master locations. The method for computing sensitivity coefficients of pressure has been developed previously, i.e., they are obtained as part of single phase flow simulation run.<sup>17</sup> The sensitivity coefficients of fractional flow rate are computed by a fast streamline-based approach, i.e., they can be obtained by simply book-keeping streamlines in the simulation field by using the 1D analytical flow solution along streamline.<sup>21</sup> The key assumption for this method is that streamline geometry is relatively insensitive to small perturbations of the permeability field that are generated within any one outer SSC iteration loop.

In the following sections, we will first briefly review the method for computing sensitivity coefficients of fractional flow rate with the streamline-based method. This method is then implemented in the SSC inversion to construct reservoir permeability models that match the observed pressure and fractional flow rate field data, while preserving consistency with the spa-

tial statistics. A synthetic example is used to demonstrate the efficiency and accuracy of this approach. The importance of integrating fractional flow rates is illustrated by comparing the inverse results using different data sets to the true reference fields. The accuracy and uncertainty of reservoir performance predictions are compared as well.

### Computation of Sensitivity Coefficients

As stated above, an efficient method for obtaining the sensitivity coefficients is key for fast and feasible inversion. A fast streamline-based method for computing the sensitivity coefficients was presented in detail in our previous paper.<sup>21</sup> Here, we summarize the analysis. Under the streamline-based flow simulation framework, the completed set of sensitivity coefficients of fractional flow rates at all master points can be obtained simultaneously by using a 1D analytical solution along streamlines. This 1D analytical solution expresses the relationship between the fractional flow rate and time-of-flight of the streamline. The permeability perturbations at all master locations are considered jointly in the calculation of sensitivity coefficients. (In the current implementation, we assume that the porosity is known, and we consider two phase flow with unit mobility ratio and matched density). The fractional flow rate for a given production well  $w_f$  at time  $t_f$  is expressed as:<sup>1</sup>

$$f(w_f, t_f) = \frac{\sum_{s=1}^{n_{w_f}^{sl}} q_s^{sl} f_s^{sl}(t_f)}{\sum_{s=1}^{n_{w_f}^{sl}} q_s^{sl}} \quad (2)$$

where  $q_s^{sl}$  is the total flow rate associated with streamline  $s$ , and  $f_s^{sl}(t_f)$  is the fractional flow rate of streamline  $s$  at time  $t_f$ .  $n_{w_f}^{sl}$  is the total number of streamlines arriving to well  $w_f$ . The derivative of  $f(w_f, t_f)$  with respect to the permeability perturbation at master point  $j$  is then:

$$\frac{\partial f(w_f, t_f)}{\partial \Delta k_j} = \frac{1}{\sum_{s=1}^{n_{w_f}^{sl}} q_s^{sl}} \sum_{s=1}^{n_{w_f}^{sl}} q_s^{sl} \frac{\partial f_s^{sl}(t_f)}{\partial \Delta k_j} \quad (3)$$

The fractional flow  $f_s^{sl}(t_f)$  along a streamline  $s$  is a function of time-of-flight of the streamline  $\tau_s$ . For tracer flow (unit mobility ratio and matched fluid density), the analytical form of  $f_s^{sl}(t_f)$  is:

$$f_s^{sl}(t_f) = \begin{cases} 1, & \text{if } \tau_s \leq t_f \\ 0, & \text{if } \tau_s > t_f \end{cases} \quad (4)$$

which can be approximated by a Gaussian cumulative function as:

$$f_s^{sl}(t_f) \approx 1 - F\left(\frac{\tau_s}{t_f}\right) \quad (5)$$

hence,

$$\frac{\partial f_s^{sl}(t_f)}{\partial \Delta k_j} = -\frac{1}{t_f} G\left(\frac{\tau_s}{t_f}\right) \frac{\partial \tau_s}{\partial \Delta k_j} \quad (6)$$

$G\left(\frac{\tau_s}{t_f}\right)$  is the Gaussian distribution function with mean 1 and small ( $< 0.001$ ) variance.

Thus, the sensitivity coefficient of fractional flow rate is the function of sensitivity coefficients of time-of-flight of all streamlines. It can be shown that the sensitivity coefficient of time-of-flight of streamline  $s$  to the permeability perturbation at master point  $j$  is the following,<sup>20</sup> see Figure 1:

$$\frac{\partial \tau_s}{\partial \Delta k_j} = \sum_{c=1}^{n_{s,c}} \left\{ \sum_{g=1}^4 \frac{\partial \Delta \tau_{s,c}}{\partial T_{0g}} \frac{\partial T_{0g}}{\partial \Delta k_j} + \sum_{l=0}^4 \frac{\partial \Delta \tau_{s,c}}{\partial p_l} \frac{\partial p_l}{\partial \Delta k_j} \right\} \quad (7)$$

where  $\Delta \tau_{s,c}$  is the time-of-flight of streamline  $s$  crossing cell  $c$ .  $T_{0g}$ ,  $g = 1, \dots, 4$ , are the transmissibilities for the four interfaces of cell 0 intersected by streamline  $s$ ,  $p_l$ ,  $l = 0, 1, \dots, 4$ , are the pressure at the cell 0 and its surrounding cells.  $\frac{\partial \Delta \tau_{s,c}}{\partial T_{0g}}$  and  $\frac{\partial \Delta \tau_{s,c}}{\partial p_l}$  can be computed from the semi-analytical expressions of time-of-flight crossing a cell.<sup>5,11</sup>  $\frac{\partial p_l}{\partial \Delta k_j}$  is the sensitivity coefficient of pressure with respect to permeability change at master location  $j$ .

Hence, the calculation of sensitivity coefficients of fractional flow is reduced to a simple book-keeping exercise for streamlines, which is both mathematically simple and computationally fast. The completed set of required sensitivity coefficients are obtained simultaneously within a single simulation run. More importantly, the spatial correlation of permeability perturbations at multiple master locations is accounted for. This method was shown to be substantially faster and more accurate than the more traditional perturbation method.<sup>20</sup>

The main features of this new method may be summarized as follows:

1. The fractional flow rate at a production well is the sum of the fractional flow rate of all contributing streamlines.
2. The sensitivity coefficient of fractional flow rate for each streamline is a function of sensitivity coefficient of time-of-flight and a derivative of the 1D analytical solution along the streamline.
3. The sensitivity coefficient of time-of-flight is separated into a pressure part and a permeability part along the streamline. The pressure part comes from a single phase flow solution, which can be obtained as part of the single phase flow simulation run. The permeability part comes from the kriging algorithm used to propagate the permeability perturbation to all grid cells.
4. The derivatives of time-of-flight with respect to transmissibility and pressure are obtained from the analytical expression of time-of-flight of the streamline.

This method has been implemented within the SSC framework. The current implementation considers unit mobility ratio and matched fluid density. A finite-difference method is used to solve the single phase flow equation for pressure field and sensitivity coefficients of pressure at all cells in the model. Master point locations are randomly selected with their locations changed every few (3-4) outer iterations. The flow equations are

solved, and the streamline geometries are updated every outer iteration.

Note that this method can be extended to compute the sensitivity coefficients of saturation when inverting saturation data. It can also be extended to compute the sensitivity coefficients to porosity if we are interested in inverting porosity field from production data. Also application of the proposed method in more practical multiphase flow conditions is possible, such as two-phase immiscible displacement, three phase flow, compositional flow, or when well conditions change during the course of production.<sup>1</sup>

### Example

In this section, we demonstrate the applications of this streamline-based SSC inverse method using a synthetic reservoir model. We compare matches of production data from permeability models inverted from pressure data only, fractional flow rate data only, and pressure and fractional flow rate data together.

Figure 2 shows a 2-D reference field (50×50 grid with cell size 20 feet × 20 feet) and the corresponding fractional flow data at four producing wells. The injection rate at the central well is 1600 STB/day, and the production rate for the 4 producing wells is 400 STB/day/well. This synthetic field was generated by using the Sequential Gaussian Simulation code, *sgsim*.<sup>6</sup> The porosity is kept constant as  $\phi = 0.2$ . Other reservoir parameters are: thickness  $h = 100$  feet, viscosity  $\mu = 0.3$  cp, and compressibility  $c = 10^{-5}$  1/psi. The main spatial variation features in this reference field to note are: (1) a high permeability zone and a low permeability zone in the middle of the field; (2) high interconnectivity between the injection well (W5) and producing well W3; (3) low interconnectivity between the injection well and producing wells W2 and W4.

Pressure data at the five wells and the fractional flow rates at the four production wells up to 1800 days (dashed line in Figure 2) are used for inverting the permeability model. Figure 3 shows three initial permeability fields (top row) and the resulting fields updated by SSC for three cases: inversion of pressure data only at the five wells (second row), inversion of fractional flow rate data only at the four production wells (third row), and joint inversion of pressure and fractional flow rate data (fourth row). The reference field is given at the bottom for comparison. The decreases of the two components of the objective function with number of iterations for the three realizations are given in Figure 4. The same 25 randomly selected master points are used for all realizations. The variogram calculated from the exhaustive reference field is used for propagating the perturbations from the master locations to the entire field. The reference histogram is explicitly honored in all updated realizations. Twenty SSC iterations are used for obtaining the final permeability models in all realizations. The CPU time for generating one realization is about 10 minutes (SGI Indigo workstation) for the case of matching both pressure and fractional flow rate data together (i.e., the fourth row in Figure 3). Less CPU time is required when matching either pressure or fractional flow rate data alone.

From Figure 3, we see qualitatively that the initial perme-

ability realizations that are generated with *sgsim* using the correct variogram and histogram poorly reproduce the reference field. As the initial models are updated by conditioning to production data, the model representation improves. The closest results are those inverted jointly from both pressure and fractional flow rate data (the third row of Figure 3). Figure 4 gives a quantitative comparison of the objective function convergences for the updated models. When only pressure data are used to invert the permeability field (first row), the fractional flow component of the objective function is not reduced to low values. Similarly, when only fractional flow rate data are used to invert the permeability field, the pressure component of the objective function is not reduced to low values. It is only when both pressure and fractional flow rate data are inverted jointly that the resulting permeability models closely reproduce both pressure and fractional flow rate data, i.e. both components of the objective function monotonically decrease to close zero (third row).

Figure 5 compares simulated and observed pressure and fractional flow rate data corresponding to the initial model and each of the converged cases for the first realization of Figure 3. For the initial permeability model, both pressure and fractional flow rate data are very poorly matched (first row). When only pressure data are used, the pressure data are almost exactly matched but fractional flow rate data are poorly matched (second row). And when only fractional flow rate data are used, the fractional flow rate are matched fairly well, but the pressure data are poorly matched (third row). Both pressure and fractional flow rate data are accurately matched when both data sets are jointly used to constrain the model (fourth row).

An overall comparison of the inverse results from the different cases is given by the ensemble fields calculated from 200 realizations, see Figure 6. For the initial fields, no additional spatial information is retained in the ensemble fields except the mean (6.0) and variance (3.0) everywhere. When pressure data alone are inverted, there is reduced uncertainty in the areas immediate to the well locations (second row). When the fractional flow rate data alone are inverted, the uncertainty is reduced in the interwell areas (third row), particularly in the major band of high permeability, i.e. with the best well response. Of course, the lowest uncertainties over more of the interwell region are obtained when both pressure and fractional flow rate data are inverted (fourth row). The joint inversion leads to reproduction of the major spatial variation features in the reference field with much less uncertainty as compared to the other two cases.

**Sensitivity to initial models and variograms** To test and illustrate the robustness of the inverse algorithm to different input models, we use the previous example reference field and start from initial models that have completely different features from the reference field, then use SSC to update them to match the pressure and fractional flow rate data. We also investigate the sensitivity of the inverse results to two different variograms.

Figure 7 shows three models updated from an uniform permeability field and two purely random permeability fields. The relative decreases of both components of the objective function are also given at the bottom row of this figure. The three final updated models (after 20 SSC iterations, using the refer-

ence field variogram) reproduce the spatial variation patterns of the reference field very well as shown on the top of the figure. The model updated from the uniform initial model displays smoother variations than the true field, while the models updated from the purely random initial fields display more fuzzy small scale features with the correct large scale patterns. All updated models accurately match both the pressure and fractional flow rate data with objective functions close to zero.

Figure 8 shows the inverse results updated from an uniform initial field with quite different anisotropic variograms: one variogram with the major correlation in the vertical direction, and the other with the major correlation in the horizontal direction. Although the final results have a different appearance than the reference field, due to the variogram structure, they both still correctly identify the relative locations of high and low permeability regions, as well as the spatial inter-connections between well pairs. Both pressure and fractional flow rate data are matched in both models with good convergence.

Thus the method is robust to the initial model and its underlying variogram structure.

**Value of additional well data** To illustrate the added value of additional data, we use the same reference model as above, but add production data from four wells in a nine-well pattern. Pressure data from the nine wells and fractional flow rate data up to 1800 days from the eight production wells are used for inversion. The two inverted permeability fields, the ensemble fields of mean and standard deviation from 200 initial field realizations are shown in Figure 9. These models reproduce the reference permeability model with much less uncertainty as compared to the results with data from five wells (Figure 3). Thus, additional well data, as expected, yield more constrained inverse results.

## Predictions of Reservoir Performance

In the previous sections, we compared the quality of the matching of pressure and fractional flow rate data with the historical data. In this section, we compare reservoir performance predictions from inverted fields with the performance of the reference model. We use the five-well synthetic example cases to predict the fractional flow at the four production wells up to 6600 days with the same well conditions (i.e., the same injection and production rate as used to match the models).

The first case is that of the initial fields where neither pressure data nor fractional flow rate data are matched. Figure 10 shows the predictions for fractional flow at the 4 production wells from 30 realizations. The solid lines are the results from the reference field. The predictions are poor, being neither accurate nor precise.

Figure 11 shows the predicted fractional flows for 30 realizations when the pressure data at the five wells are matched. There is clear improvement compared to the initial fields. However, these predictions are still somewhat poor in accuracy and have large uncertainty. This indicates that matching single phase pressure data may not be sufficient for reliable prediction of multiphase flow: more information is required.

When the permeability models match the fractional flow

rate data up to 1800 days at the four wells, the predictions are shown in Figure 12. The predictions of fractional flow at the four wells are dramatically improved. This is because the same type of early time data at the same wells are matched.

The best predictions of reservoir performance are obtained by using the reservoir models in which both pressure and fractional flow rate data (again up to 1800 days) at the same wells are matched, see Figure 13. Note that incorporating pressure data when matching fractional flow rate data yields a better match of fractional flow rate than using only fractional flow rate data (compare the matches for fractional flow rates before 1800 days in Figures 11 and 12).

Next, we investigate the results for reservoir performance predictions for a set of wells which were not included in the production data inversion. Using the synthetic example with the nine-well pattern, we predict the fractional flow rate at wells 6 to 9 (up to 6600 days) using the permeability realizations generated by matching pressure and fractional flow rate data at wells 1 to 5 (up to 1800 days only), see Figure 9. Figures 14 and 15 show the histograms of the first water breakthrough times and times of 80% watercut predicted at wells 6 to 9 from 200 realizations: the left hand side histograms are from initial permeability fields in which no production data are matched; the right hand side histograms are from the permeability fields that match pressure and fractional flow rate data at wells 1 to 5.

Predictions from the initial realizations with no production data matched are inaccurate with large uncertainty. When the pressure data at wells 1 to 5 and the fractional flow rate data at wells 1 to 4 are integrated, the resulting predictions at wells 6 to 9 are improved considerably. This improvement, however, is not as dramatic as compared to the previous example when the early production data at the same wells being predicted are matched. A number of factors will influence the ability to predict performance from wells, such as infill, side-track, or step-outs, based on inversion of production data from another set of wells. These factors include the well spacing, reservoir heterogeneity, the frequency and accuracy of the pressure and flow breakthrough data.

### Summary and Future Work

The SSC method<sup>21</sup> for inverting pressure data at wells to multiple realizations of reservoir permeability has been extended for inversion to match historical pressure and multiphase fractional flow rate data. Adaptation of a streamline-based multiphase flow simulator for fast forward simulation, and development of an efficient methodology of computing the sensitivity coefficients of fractional flow rate to permeability were the keys to the new method. This new method decouples the multiple-dimensional flow problem into multiple 1D problems along streamlines. Using the analytical 1D flow solution along the streamline, the completed set of sensitivity coefficients of fractional flow rate are obtained simultaneously by book-keeping all streamlines with only **one** single phase flow simulation. A consequence of the approach is that the perturbations at all master locations are jointly considered through kriging, which improves the accuracy and robustness.

Applications of the extended SSC method were demon-

strated using a synthetic example. Comparisons were made among the results inverted from different sets of production data: pressure data only, fractional flow rate data only, and both pressure and fractional flow rate data.

Results show that production data carry important information on the spatial variation of reservoir properties, and more spatial variation patterns can be identified with less uncertainty by integrating more production data. While pressure data carry information on relatively large scale trends around the well, fractional flow rate data provide additional information on the spatial connectivity between well pairs. Matching pressure or fractional data alone can result in high uncertainty in the inverse results. Integrating both pressure and fractional flow rate data jointly significantly improves the reservoir heterogeneity representation over those when only pressure or fractional flow rate data are matched alone.

Dramatic improvement in reservoir performance predictions is observed when production data are integrated with more accurate predictions and less uncertainty. Results from this study also show that:

- matching pressure data, although improving the prediction results, may not be sufficient for reliable predictions of fractional flow, even at the same wells in which the pressure data are matched.
- good reservoir performance predictions can be obtained when the early time production data at the same wells with similar flow and well conditions are matched.
- poor predictions may be obtained when the early time production data at the wells being predicted are not integrated, or well and flow conditions are changed between the calibration stage and prediction stage. This is particularly true when the number of wells used for conditioning is small and is consistent with the findings by Huang et al.<sup>9</sup>

Future work includes:

- Extend the algorithm to true two- or three-phase flow that handles mobility changes during the course of production. In such cases, pressure solution and thus streamline geometry need to be updated with time through the simulation. The number of pressure solutions required will depend on the degree of nonlinearity of the problem. Studies have shown that only a few pressure solutions are sufficient for most displacement problems dominated by the heterogeneity of reservoir properties.<sup>1,14</sup>
- Provide changing well conditions, such as infill and recompletions, over the production history.
- Extend to full 3D to model production from multilayer reservoirs with production rate profiles along the borehole.
- Extend the streamline-based method to integrate saturation data from production wells or even from 4D seismic data.<sup>10</sup>

## Acknowledgement

We thank Mobil Oil Strategic Research Center and the Stanford Center for Reservoir Forecasting for making this research possible.

## Nomenclature

$p$	=	pressure, psi
$f$	=	fractional flow rate
$t$	=	time, day
$\tau$	=	time-of-flight, day
$k$	=	permeability, md
$O$	=	objective function
$n_m$	=	number of master points
$n_{wp}$	=	number of wells with pressure data
$n_{tp}$	=	number of time steps for pressure
$W_p$	=	weight assigned to pressure data
$n_{wf}$	=	number of wells with fractional flow rate data
$n_{tf}$	=	number of time steps for fractional flow rate
$W_f$	=	weight assigned to fractional flow rate data

## References

1. R. P. Batycky. *A Three-Dimensional Two-Phase Field Scale Streamline Simulator*. PhD thesis, Stanford University, Stanford, CA, 1997.
2. R. P. Batycky, M. J. Blunt, and M. R. Thiele. A 3D field-scale streamline-based reservoir simulator. *SPE Reservoir Engineering*, November:246–254, 1997.
3. M. J. Blunt, K. Liu, and M. R. Thiele. A generalized streamline method to predict reservoir flow. In *8th European Symposium on Improved Oil Recovery*, pages 269–278, Vienna, Austria, May 1995.
4. J. E. Capilla, J. J. Gómez-Hernández, and A. Sahuquillo. Stochastic simulation of transmissivity fields conditioning to both transmissivity and piezometric data, 2. demonstration in a synthetic case. *Journal of Hydrology*, 203:175–188, 1998.
5. A. Datta-Gupta and M. J. King. A semianalytic approach to tracer flow modeling in heterogeneous permeable media. *Adv. in Water Resources*, 18(1):9–24, 1995.
6. C. V. Deutsch and A. G. Journel. *GSLIB: Geostatistical Software Library and User's Guide*. Second Edition, Oxford University Press, New York, 1997.
7. J. J. Gómez-Hernández, A. Sahuquillo, and J. E. Capilla. Stochastic simulation of transmissivity fields conditional to both transmissivity and piezometric data, 1. The theory. *J. of Hydrology*, 203:162–174, 1998.
8. Wences P. Gouveia, A. S. Cullick, and Clayton V. Deutsh. An optimization framework for reservoir characterization. In *SEG Annual Meeting*, New Orleans, Nov. 1998.
9. X. Huang, A. Gajraj, and M. Kelkar. The impact of integrating static and dynamic data in quantifying uncertainty in the future prediction of multiphase systems. *SPE Formation Evaluation*, pages 263–269, Dec. 1997.
10. J. L. Landa. *Reservoir Parameter Estimation Constrained to Pressure Transients, Performance History and Distributed Saturation Data*. PhD thesis, Stanford University, Stanford, CA, 1997.
11. D. W. Pollock. Documentation of computer programs to compute and display pathline results from the US geological survey modular three-dimensional finite-difference ground-water flow model. Technical Report Open File Report 89-381, U.S. Geological Survey, 1989.
12. N-Z. Sun. *Inverse Problems in Groundwater Modeling*. Kluwer Academic Publishers, Boston, 1994.
13. A. Tarantola. *Inverse Problem Theory: Methods for Data Fitting and Model Parameter Estimation*. Elsevier, Amsterdam, The Netherlands, 1987.
14. M. R. Thiele. *Modeling Multiphase Flow in Heterogeneous Media Using Streamtubes*. PhD thesis, Stanford University, Stanford, CA, 1994.
15. M. R. Thiele, M. J. Blunt, and F. M. Orr. Predicting multicomponent, multiphase flow in heterogeneous systems using streamtubes. In *4th European Conference on the Mathematics of Oil Recovery*, Roros, Norway, June 1994.
16. X. H. Wen. *Geostatistical Methods for Prediction of Mass Transport in Groundwater*. PhD thesis, Royal Institute of Technology, Stockholm, Sweden, 1995.
17. X. H. Wen, C. V. Deutsch, and A. S. Cullick. High resolution reservoir models integrating multiple-well production data. In *1997 SPE Annual Technical Conference and Exhibition Formation Evaluation and Reservoir Geology*, pages Part 2, 115–129, San Antonio, TX, October 1997. Society of Petroleum Engineers. SPE Paper Number 38728.
18. X. H. Wen, C. V. Deutsch, and A. S. Cullick. A review of current approaches to integrate flow production data in geological modeling. In *Report 10, Stanford Center for Reservoir Forecasting*, Stanford, CA, May 1997.
19. X. H. Wen, C. V. Deutsch, and A. S. Cullick. A short note on spatial constraints on permeability due to permanent pressure gauge/multiple well test data. In *Report 10, Stanford Center for Reservoir Forecasting*, Stanford, CA, May 1997.
20. X. H. Wen, C. V. Deutsch, and A. S. Cullick. Facies proportion maps from well production data. *SPEJ*, 1998. Submitted.
21. X. H. Wen, C. V. Deutsch, and A. S. Cullick. A fast streamline-based method for computing sensitivity coefficients of fractional flow rate. *SPEJ*, 1998. Submitted.
22. X. H. Wen, J. J. Gómez-Hernández, J. E. Capilla, and A. Sahuquillo. The significance of conditioning on piezometric head data for predictions of mass transport in groundwater modeling. *Math. Geology*, 28(7):961–968, October 1996.
23. D. A. Zimmerman, C. L. Axness, G. de Marsily, M. G. Marietta, and C. A. Gotway. Some results from a comparison study of geostatistically-based inverse techniques. Sandia National Laboratories, Albuquerque, NM, 1995.

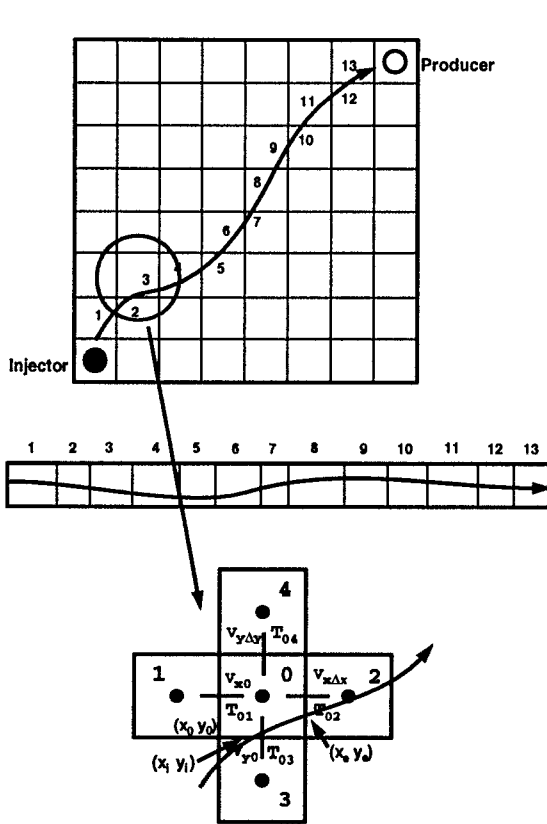


Figure 1: Schematic for tracking a streamline in a discretized numerical model.

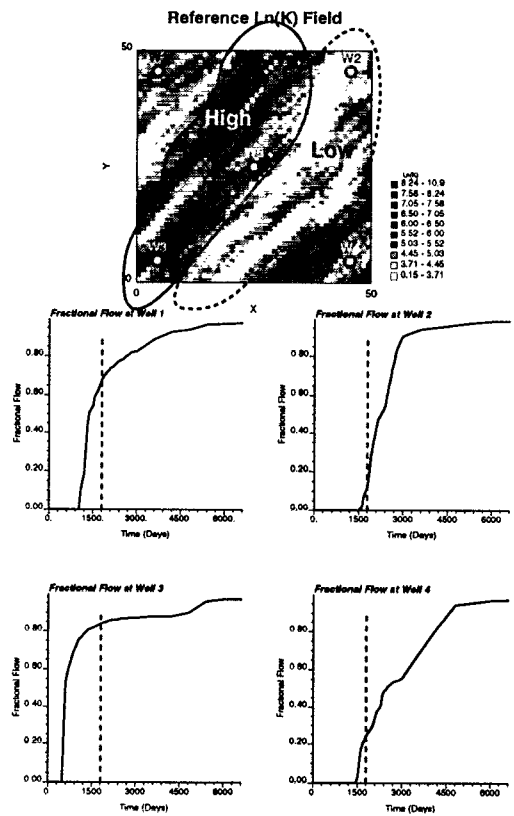


Figure 2: Synthetic, stochastic reference field and the fractional flow rate data from the four corner wells.

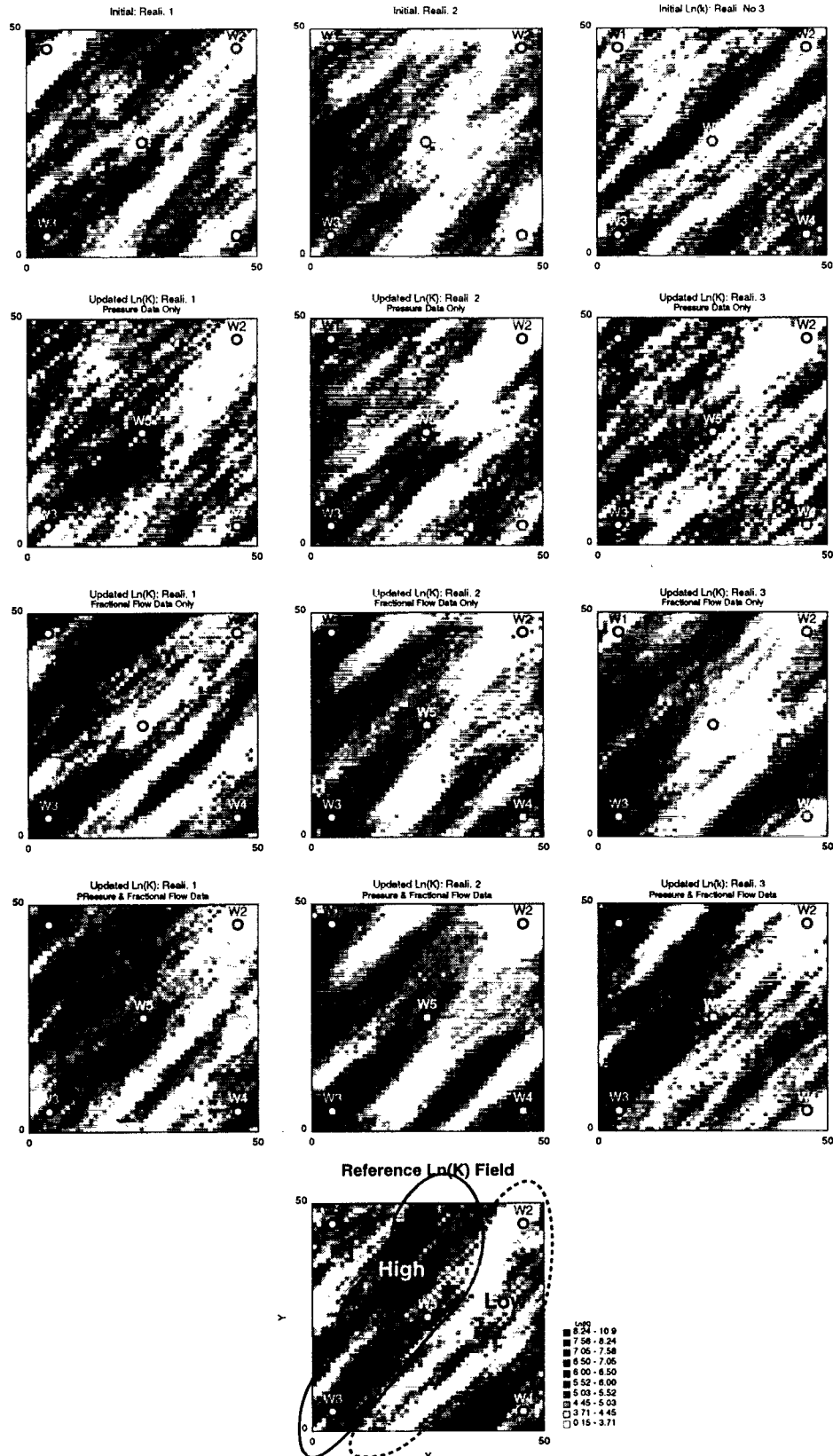


Figure 3: Three initial realizations and the corresponding models updated by the SSC method with inversion on pressures only, fractional flows only, and both.

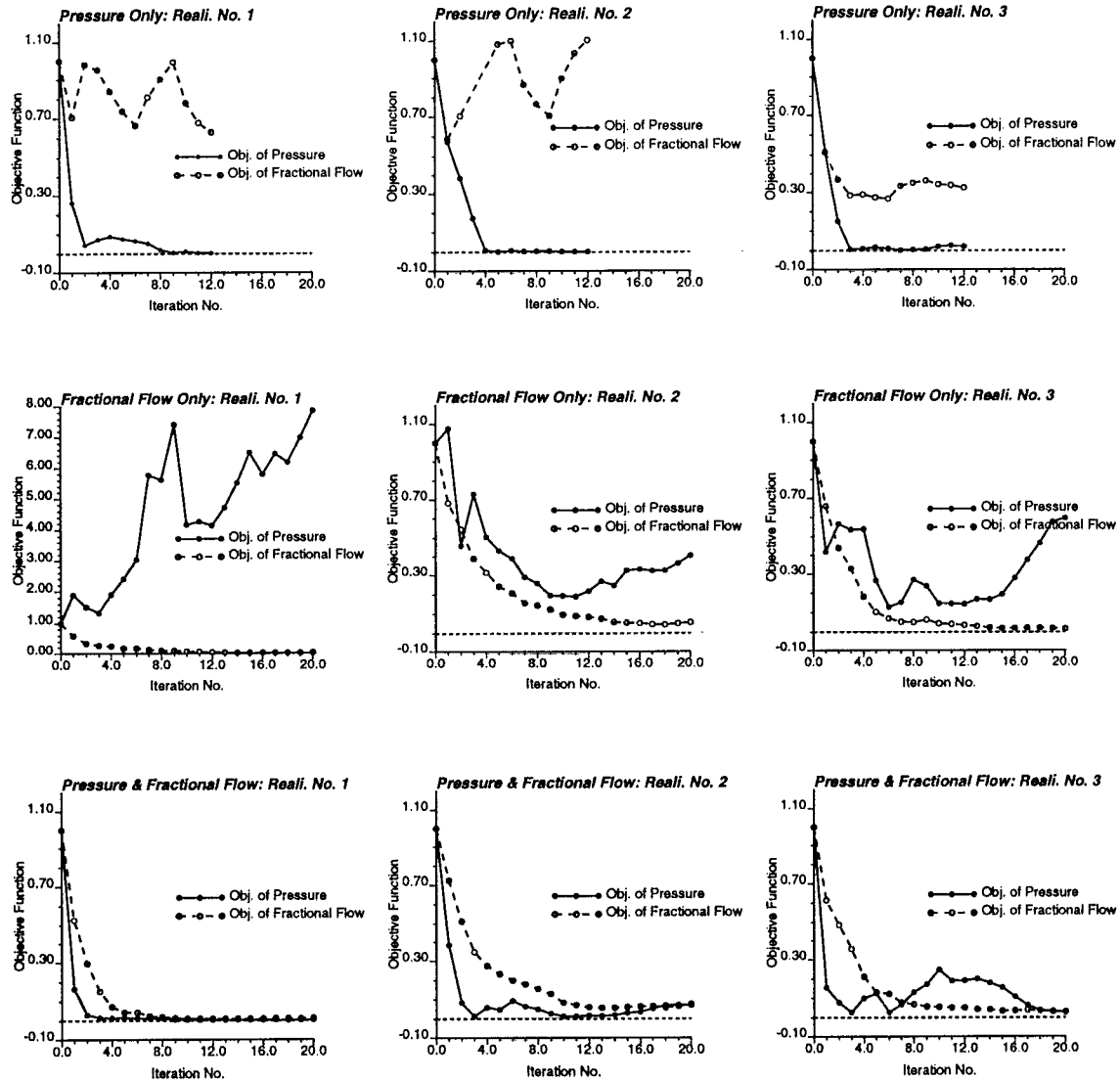


Figure 4: Decrease of objective function for the three realizations with inversion on pressures only, fractional flows only, and both.cases.

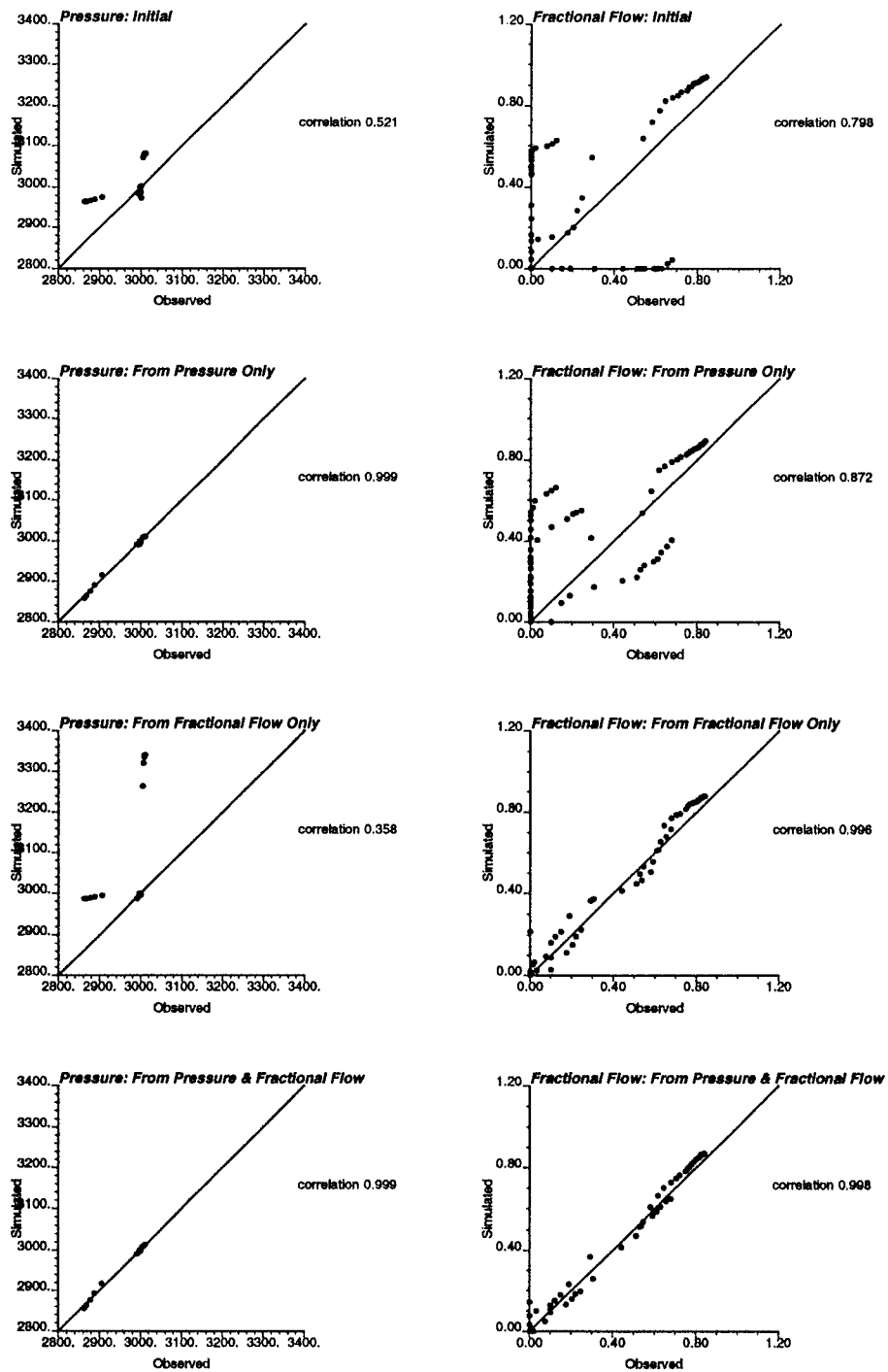


Figure 5: Comparison of match of pressures and fractional flows (for one of the initial permeability realizations), with inversion on pressures only, fractional flows only, and both.

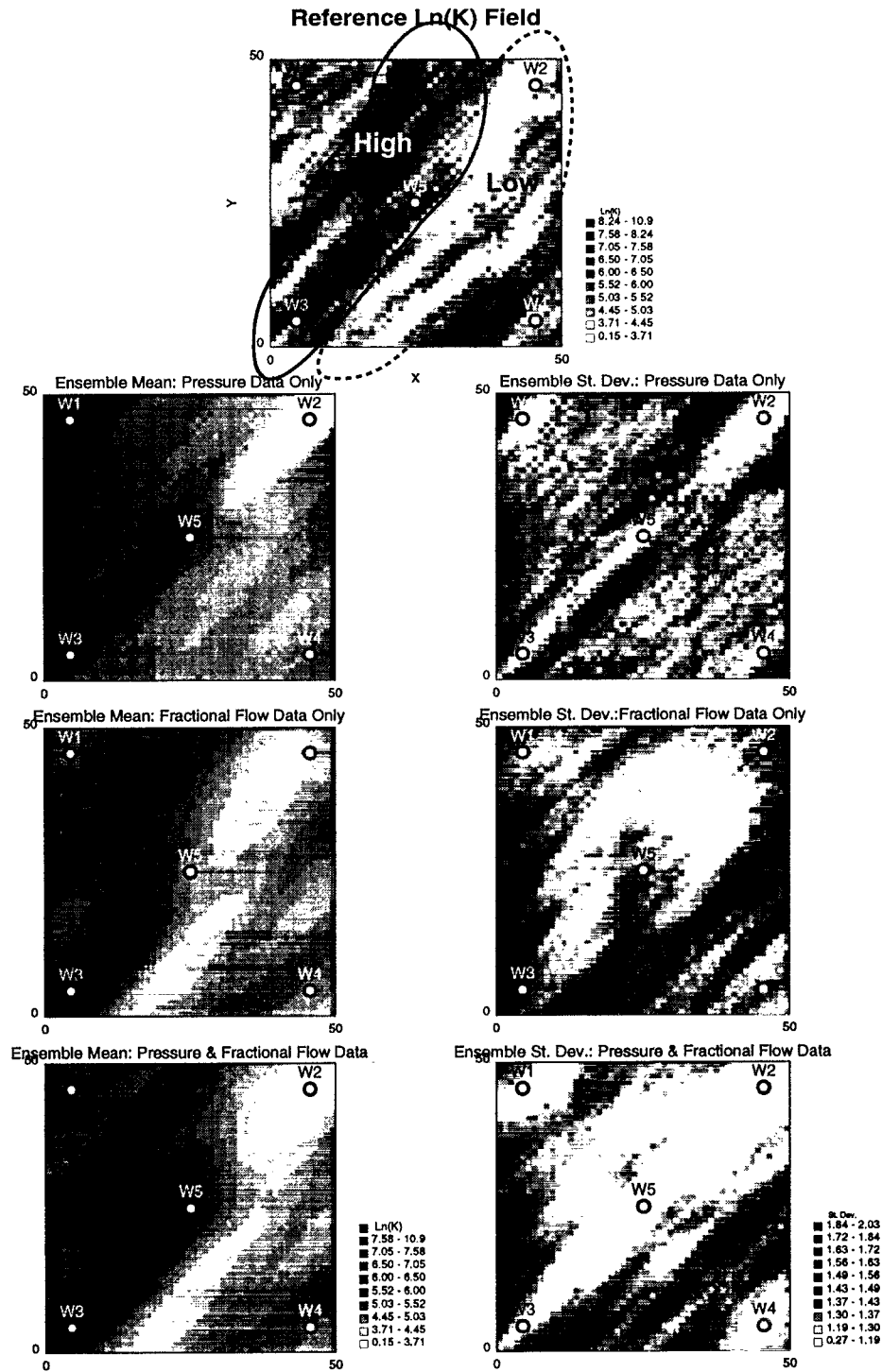


Figure 6: Ensemble means and standard deviations from 200 permeability realizations, comparing inversion on pressures only, fractional flows only, and both.

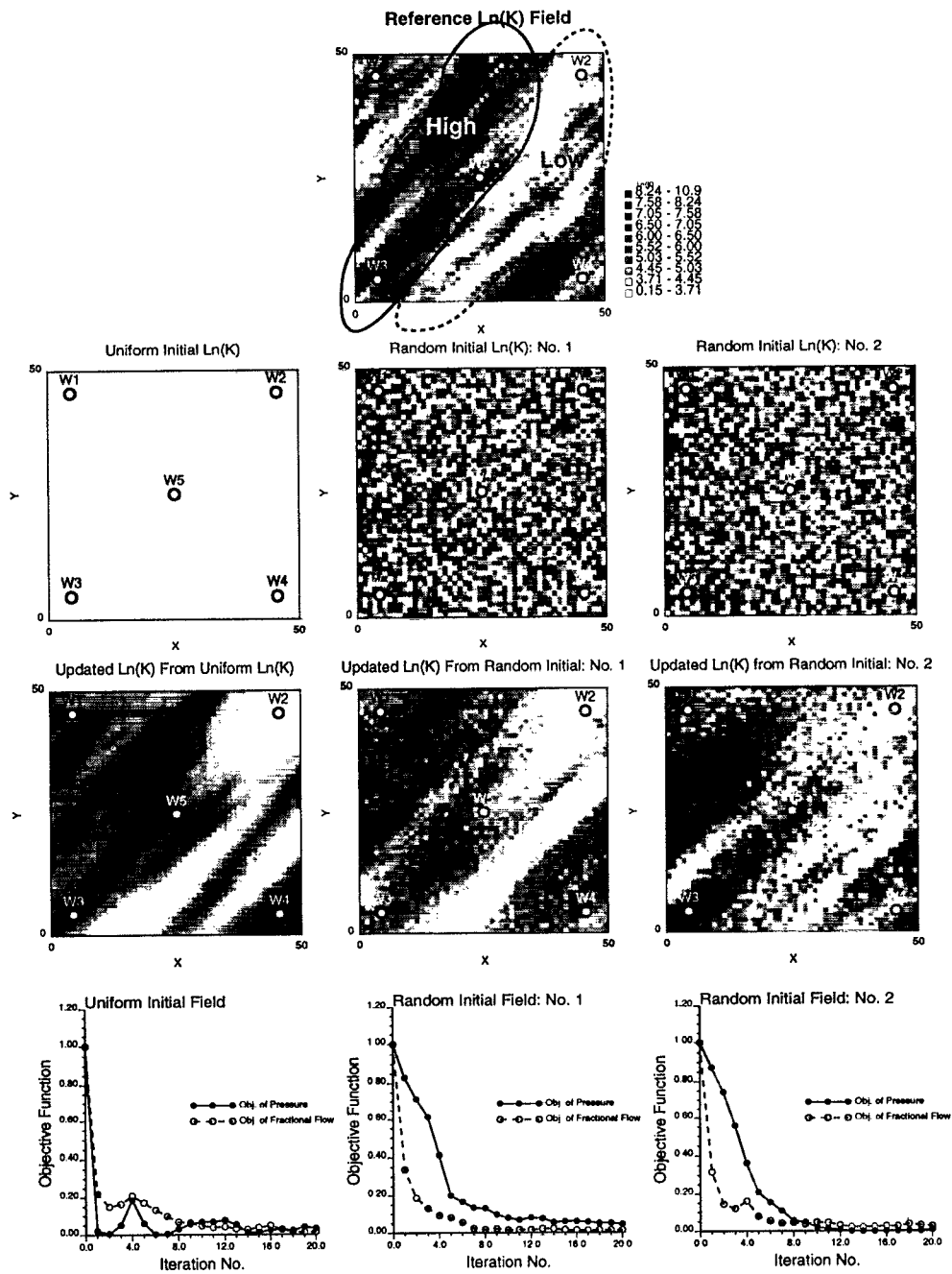


Figure 7: Comparison of the inverse results using different initial models.

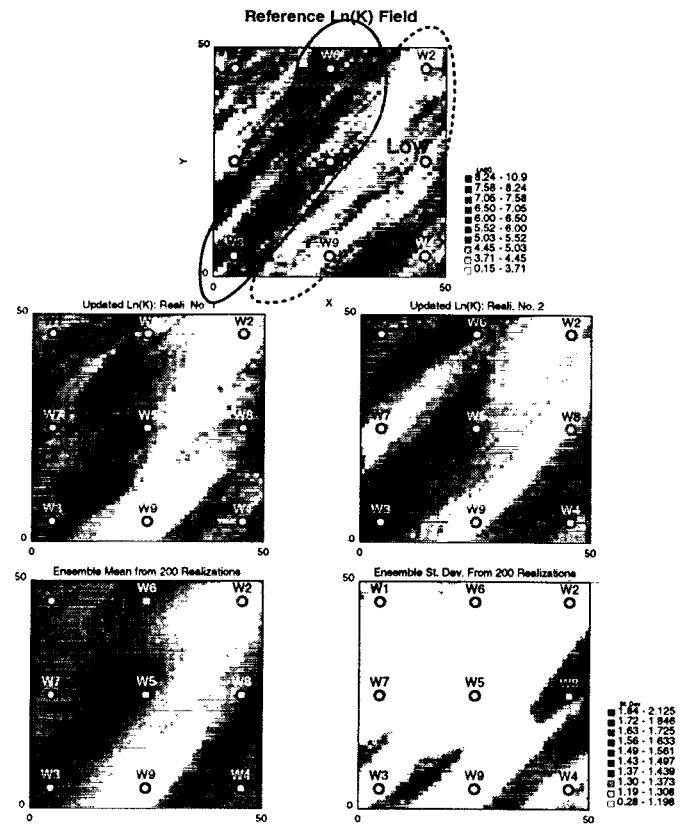
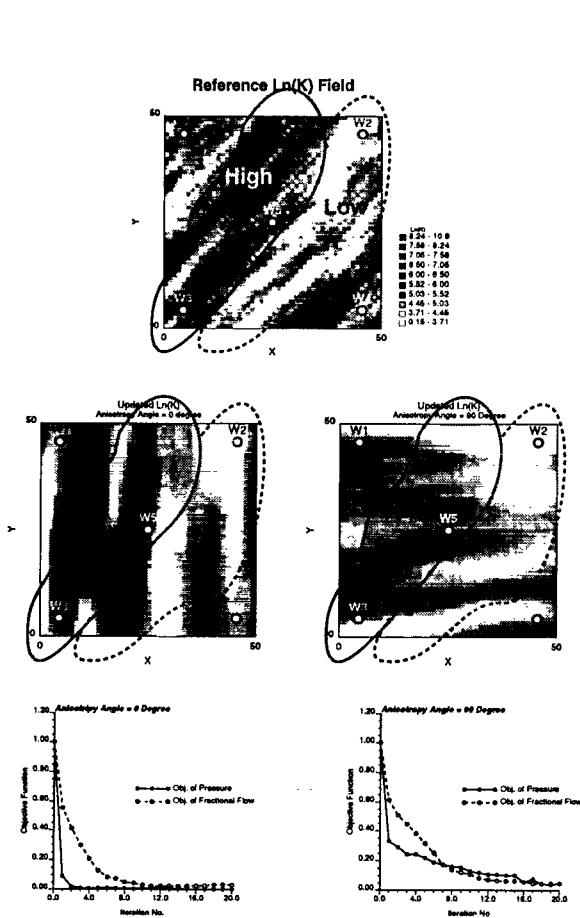


Figure 8: Comparison of the inverse results using different variogram models.

Figure 9: The reference field, two realizations of inverse results, the ensemble mean and standard deviation maps for 200 realizations when production data from 9 wells are used for inversion.

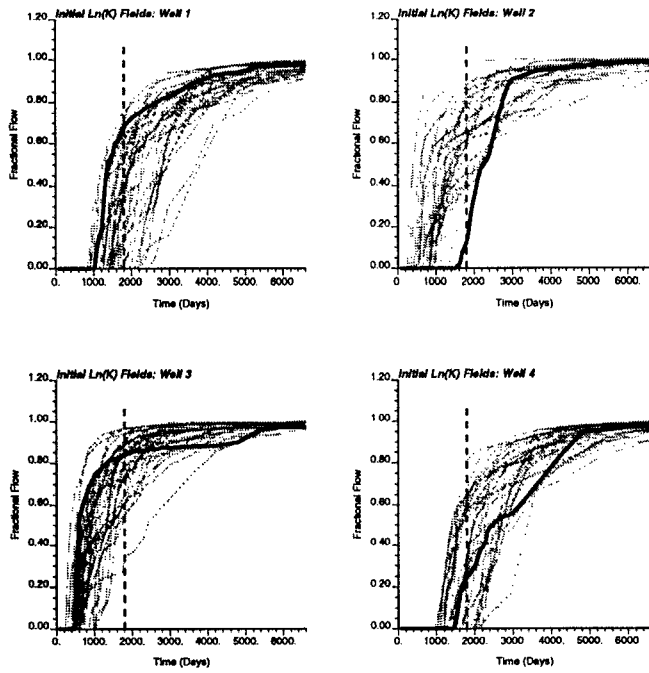


Figure 10: Fractional flow rate predictions at the four production wells from 30 initial permeability realizations. Thick lines are results from the reference field.

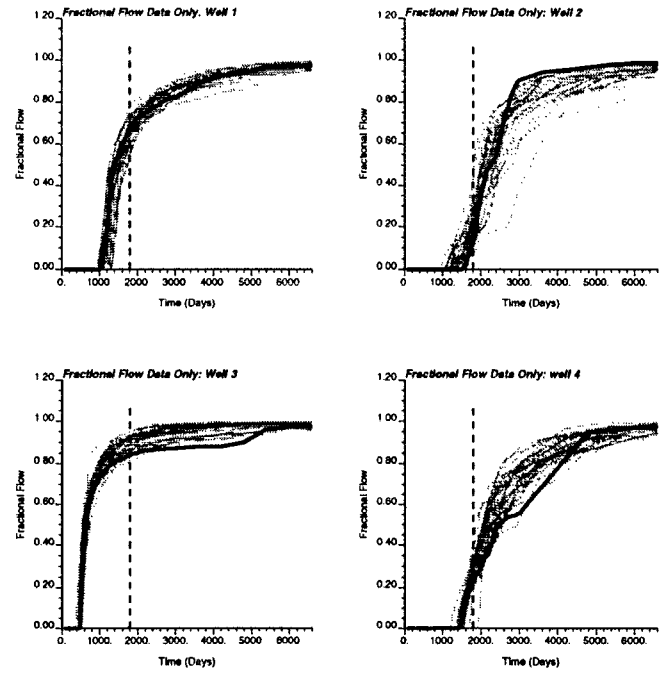


Figure 12: Fractional flow rate predictions at the four production wells from inversion of fractional flow data alone for 30 initial permeability realizations. Thick lines are results from the reference field.

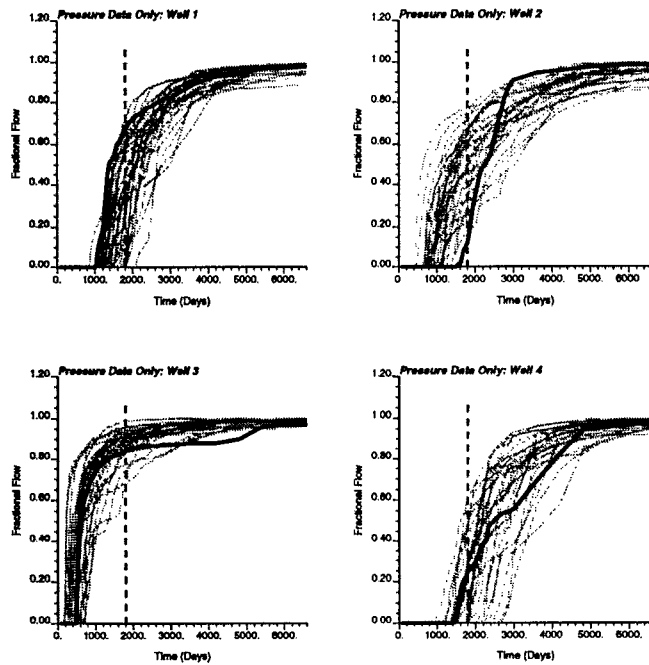


Figure 11: Fractional flow rate predictions at the four production wells from inversion of pressure data alone for 30 initial permeability realizations. Thick lines are results from the reference field.

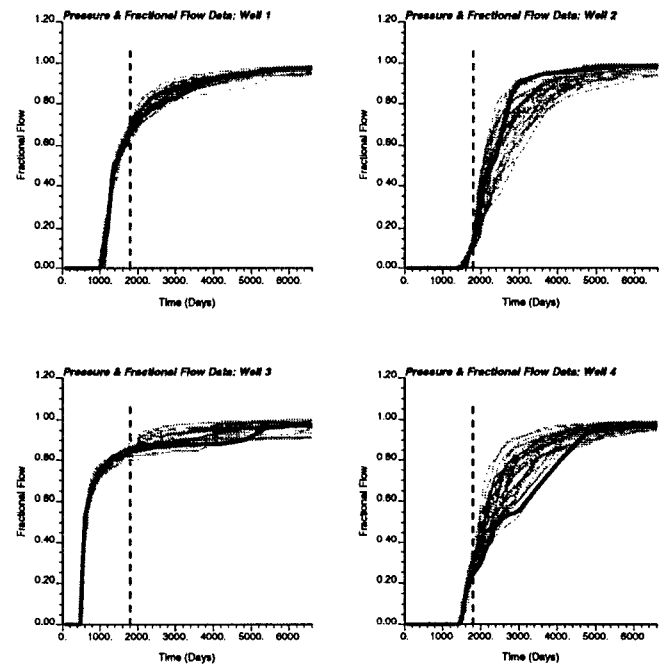


Figure 13: Fractional flow rate predictions at the four production wells from joint inversion of pressure and fractional flow data for 30 initial permeability realizations. Thick lines are results from the reference field.

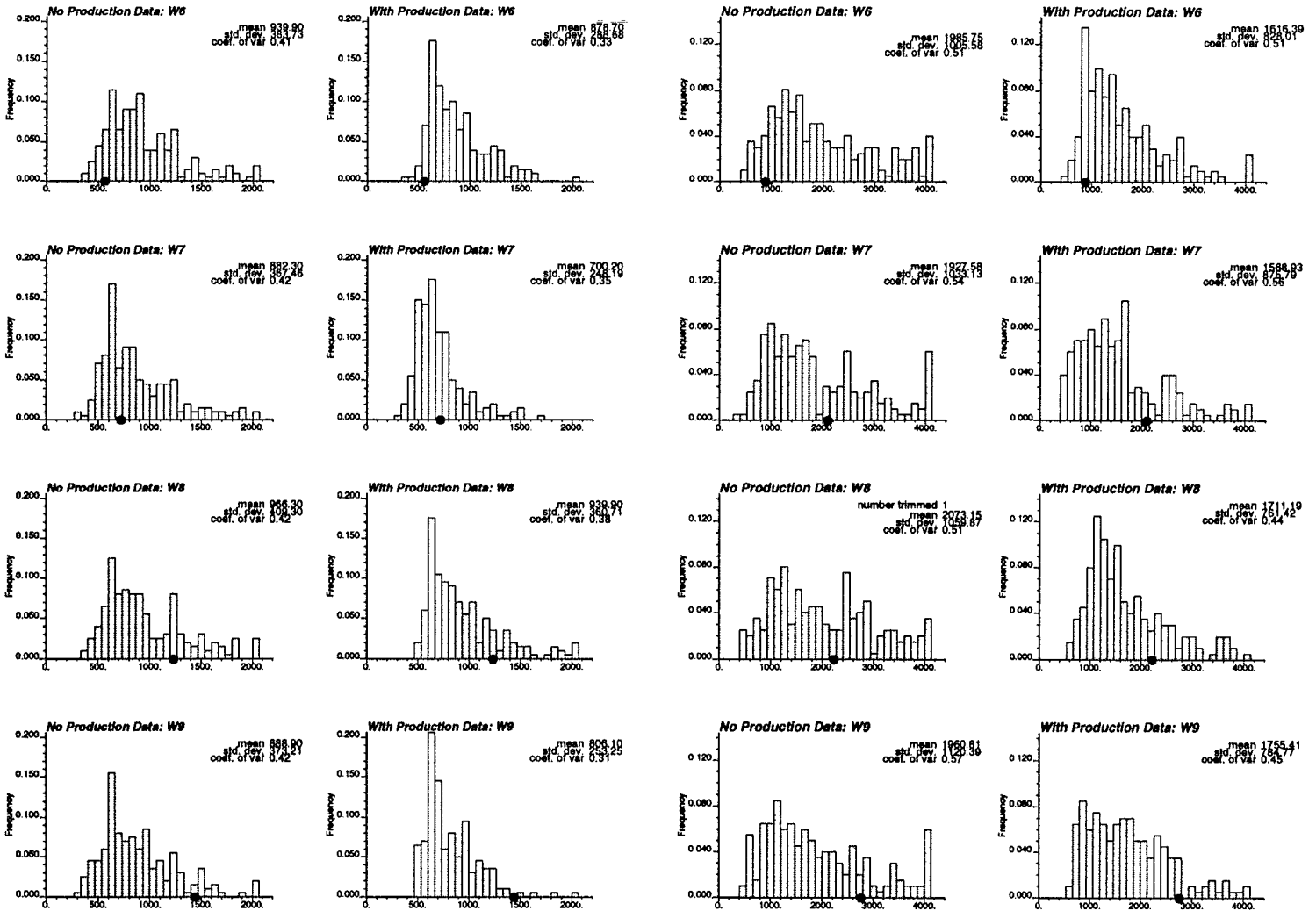


Figure 14: Comparison of the histograms of water breakthrough time predicted at wells 6 to 9 using initial permeability fields (left column) and updated permeability fields (right column) that honor pressure and fractional flow rate data at wells 1 to 5. The bullets are the true times from the reference field.

Figure 15: Comparison of the histograms of time for 80% watercut predicted at wells 6 to 9 using initial permeability fields (left column) and updated permeability fields (right column) that honor pressure and fractional flow rate data at wells 1 to 5. The bullets are the true times from the reference field.